ARL-TR-9857 ● Dec 2023

Evaluation of Microstructure and Properties of Medium-Manganese Steels Modified with Molybdenum

by Daniel M Field, Daniel J Magagnosc, Billy C Hornbuckle, Jeffrey T Lloyd, and Krista R Limmer

NOTICES

Disclaimers

The findings in this report are not to be construed as an official Department of the Army position unless so designated by other authorized documents.

Citation of manufacturer's or trade names does not constitute an official endorsement or approval of the use thereof.

Destroy this report when it is no longer needed. Do not return it to the originator.

ARL-TR-9857 ● DEC 2023

Evaluation of Microstructure and Properties of Medium-Manganese Steels Modified with Molybdenum

Daniel M Field, Daniel J Magagnosc, Billy C Hornbuckle, Jeffrey T Lloyd, and Krista R Limmer
DEVCOM Army Research Laboratory

REPORT DOCUMENTATION PAGE

1. REPORT DATE	2. REPORT TYPE	3. DATES COVERED	
		START DATE	END DATE
December 2023	Technical Report	11/01/2020	9/30/2021

4. TITLE AND SUBTITLE
Evaluation of Microstructure and Properties of Medium-Manganese Steels Modified with Molybdenum

5a. CONTRACT NUMBER	5b. GRANT NUMBER	5c. PROGRAM ELEMENT NUMBER
5d. PROJECT NUMBER	5e. TASK NUMBER	5f. WORK UNIT NUMBER

6. AUTHOR(S)
Daniel M Field, Daniel J Magagnosc, Billy C Hornbuckle, Jeffrey T Lloyd, and Krista R Limmer

7. PERFORMING ORGANIZATION NAME(S) AND ADDRESS(ES)
DEVCOM Army Research Laboratory
ATTN: FCDD-RLA-MF
Aberdeen Proving Ground, MD 21005

8. PERFORMING ORGANIZATION REPORT NUMBER
ARL-TR-9857

9. SPONSORING/MONITORING AGENCY NAME(S) AND ADDRESS(ES)	10. SPONSOR/MONITOR'S ACRONYM(S)	11. SPONSOR/MONITOR'S REPORT NUMBER(S)

12. DISTRIBUTION/AVAILABILITY STATEMENT
DISTRIBUTION STATEMENT A. Approved for public release: distribution unlimited.

13. SUPPLEMENTARY NOTES
ORCID IDs: Daniel M Field, 0000-0002-8890-4391; Daniel J Magagnosc, 0000-0002-1418-9292, Krista R Limmer, 0000-0003-4775-5876; Jeffrey T Lloyd, 0000-0002-4930-5361

14. ABSTRACT
Three medium-manganese steels with varying manganese, carbon, and aluminum levels were investigated as a function of heat treatment and molybdenum additions. Effects of alloying and heat treatment in the wrought plates were characterized through microstructure and hardness evaluation. Further examination of selected alloy conditions included tensile and Charpy v-notch impact testing. Results showed that molybdenum additions enabled simultaneous increases in both hardness and toughness—unique increases in two properties that are typically inversely correlated. The –40 °C Charpy v-notch impact properties correlated well with the quasi-static tensile reduction in area of these alloys. This correlation is also demonstrated in other medium-manganese, high-nickel, and low-alloy ultrahigh strength steels found in literature.

15. SUBJECT TERMS
medium-manganese steel, microstructure, toughness, heat treatment, austenite stability, Charpy toughness, Sciences of Extreme Materials

16. SECURITY CLASSIFICATION OF:			17. LIMITATION OF ABSTRACT	18. NUMBER OF PAGES
a. REPORT	b. ABSTRACT	C. THIS PAGE		
UNCLASSIFIED	UNCLASSIFIED	UNCLASSIFIED	UU	33

19a. NAME OF RESPONSIBLE PERSON	19b. PHONE NUMBER *(Include area code)*
Daniel M Field	(410) 306-0742

STANDARD FORM 298 (REV. 5/2020)
Prescribed by ANSI Std. Z39.18

Contents

List of Figures

List of Tables

1. Introduction

Medium manganese (5–12 wt% Mn) steels are a class of third generation advanced high-strength steels with fine-grained dual-phase microstructures of ferrite (α) and austenite (γ) that are created by cold working followed by intercritical annealing (ICA). ICA in steel is defined as a heat treatment within a two-phase (i.e., α + γ) field that promotes the partitioning of elements to stabilize the dual-phase microstructure and enables the retention of metastable γ down to room temperature. The alloying elements that stabilize the γ are substitutional manganese (Mn), and interstitial carbon (C). The metastable γ can, under the imposition of a stress or strain, transform to α-martensite and provide increased total elongation by delaying the onset of necking. This is referred to as transformation-induced plasticity (TRIP) behavior. Aluminum (Al) and molybdenum (Mo) conversely partition to the α during ICA and provide solid solution strengthening to counteract the lower strength metastable γ. These medium-Mn steels demonstrate combinations of high ultimate tensile strength and total elongation from 700 MPa with 65% elongation to 1550 MPa and 10% elongation.[1,2]

Most medium-Mn steel investigations have been limited to thin sheet steels (≤1.5 mm). Sheet processing conventionally involves hot rolling, cold rolling, and concludes with heat treatment to produce the requisite microstructure as described previously. The high reduction ratios during rolling of thin sheets result in greater homogeneity in both microstructure and composition as compared to as hot-rolled plate. For thin gauge steel sheet, Charpy v-notch (CVN) energy or quasi-static plane-strain toughness are rarely measured. Reports of toughness on these thin gauges and alloys is most often derived as the product of the ultimate tensile strength and ductility (Eq. 1), as measured by quasi-static tension tests, and is not comparative to impact toughness as measured by CVN. This tensile toughness value is generally calculated using Eq. 1 and is intended as an approximation of the area under the stress–strain curve; however, this is a gross oversimplification. This approximation assumes that the response of the steel is elastic followed by a perfectly plastic behavior, which is not the case for the high work-hardening medium-Mn alloys.

$$\text{Tensile Toughness (GPa·\%)} = \text{Ultimate Tensile Strength (MPa)} \times \text{total ductility (\%)} \quad (1)$$

The work of Niikura and Morris[3] is one of the few studies investigating the toughness; they used CVN and K_{1C} measurements, of medium-Mn (5–8 wt%) and high-nickel (Ni) steels (~9 wt%) for use in low-temperature (≤–40 °C) applications. They noted the effect of γ on improving toughness, yet there appeared to be a

maximum γ concentration of approximately 10% that improved toughness, and they noted that higher values of γ began to degrade toughness.

The effect of γ stability is also a crucial component to toughness. Recent work by Field et al.[4] showed that γ stability is the key component for promoting high –40 °C CVN values. What they identified is that as the γ volume fraction increased the γ became less enriched in stabilizing elements during ICA from a mass balance perspective. The reduced stability promoted a thermal transformation at the onset of cooling to the test temperature producing brittle fresh martensite that behaves as an easy crack propagation pathway. This novel result showed that the heat treatment producing the greatest volume of γ (33 vol%) also exhibited the higher ultimate tensile strength (890 MPa), higher tensile toughness per Eq. 1 (50.6 GPa%), but significantly lower –40 °C impact toughness (20 ft-lb) than the lower γ-containing condition (8 vol%, 730 MPa, 41.8 GPa% and 61 ft-lb, respectively).

The inclusion of carbide-forming elements is also known to influence the toughness. For instance, the effect of Mo on the toughness of traditional chromium-nickel steels is well understood yet poorly documented. Work by Nakamura et al.[5] from 1979 showed that the toughness was significantly improved as either Mo increased or C decreased. They showed that Mo could improve the toughness through a direct strengthening effect when C was low and carbides were not formed. When C was increased to 0.3 wt%, however, the toughening effect of Mo was attributed to the formation of favorable carbides like Mo_2C.

This report serves to identify the effects of heat treatment (i.e., ICA temperature and time) and alloying on the microstructure and mechanical properties in medium-Mn steels. Three different medium-Mn steel plates with and without Mo additions were evaluated after different heat treatments were applied to evolve different types of microstructures. This work was also motivated to understand how plate processing can be applied to medium-Mn steels for thicker gauge applications, beyond what has been reported in sheet steels.

2. Experimental Procedure

Each alloy in this study was vacuum induction melted and cast into a 10.2- × 45.7- × 15.2-cm^3, 120-kg ingot. The compositions of the alloys are shown in Table 1. The three base chemistries are designated by their nominal Mn and C concentrations (i.e., the alloy containing 5 wt% Mn and 0.05 wt% C is designated as "505"). Modified versions of each of the base alloys (505, 515, and 1015) were also produced by alloying with 0.5 wt% Mo. These Mo-modified alloys are designated with an "M". Composition analysis of the cast materials was obtained by inductively coupled plasma spectrometry after sample dissolution in hydrochloric

and nitric acid. C, sulfur (S), nitrogen (N), and oxygen (O) contents were determined using gas combustion analysis. The weight fractions of N and S were both less than 0.005 wt%, and O was less than 0.001 wt%. Hot rolling was performed after heating to 1200 °C and holding for 4 h. The ingot was initially rolled to a width of 30.5 cm and followed by rolling to a gauge thickness of 1.4–1.5 cm. After achieving the final gauge thickness, plates were immediately transferred to a 700 °C furnace and held at temperature for 1 h followed by air cooling.

Table 1 Composition in weight percent of the alloys under investigation; balance of composition is iron (Fe)

Alloy	Mn	C	Si	Al	Mo
505	5.01	0.05	0.19	0.19	…
505M	5.03	0.05	0.20	0.17	0.52
515	5.04	0.16	0.19	0.17	…
515M	5.08	0.16	0.19	0.18	0.53
1015	9.84	0.16	0.18	1.93	…
1015M	9.89	0.16	0.19	2.15	0.52

ICA heat treatment was performed to affect γ stability by heating to 600 or 650 °C, holding for 1 or 20 h, followed by air cooling. Phase diagrams generated using the TCFE10 database in Thermo-Calc 2020b are shown in Fig. 1, with points indicating the ICA temperatures for each alloy. At the higher ICA temperature a greater volume fraction of γ is expected to form and is anticipated to be of a lower stability compared to the lower ICA treatment temperature. The 600 and 650 °C temperatures were chosen based on the results presented in the work by Field et al.[4] that showed the kinetics for γ stability are significantly retarded in these alloys when annealing was performed below 600 °C. Following ICA treatment, a carbide temper treatment was performed for the Mo-containing alloys at either 204 or 530 °C for 2 h followed by air cooling. These conditions are referred to according to their ICA and tempering conditions as an amendment to the composition nomenclature (i.e., 505M-ICA650-1-T530 for the 650 °C, 1 h ICA and 530 °C tempered condition of the Mo-modified 5 wt% Mn 0.05 wt% C alloy. These tempering temperatures were selected to evaluate the effect of a Stage I temper at 204 °C producing carbon clustering, or formation of M_2C carbides as identified in the phase diagrams shown in Fig. 1. A summary table of the nomenclature for all alloys and heat treatments is provided in Table 2. Hardness was measured by Rockwell C and B techniques and converted to Brinell hardness (HBW) for reporting according to ASTM E18-17.[6]

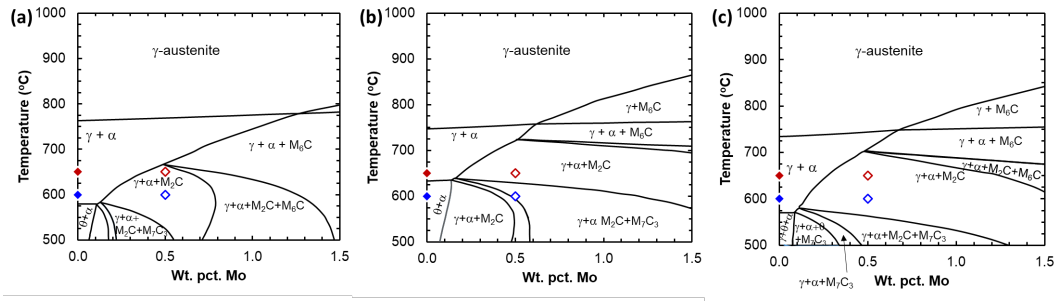

Fig. 1 Equilibrium phase diagrams of the nominal base steel composition (a) 0.05C–5Mn–0.2Si–0.2Al, (b) 0.15C–5Mn–0.2Si–0.2Al, and (c) 0.15C–10Mn–0.2Si–2.0Al with varying Mo contents. ICA treatment temperature indicated for each of the Mo contents is shown for reference.

Table 2 Nomenclature for composition, ICA conditions, and carbide tempering conditions for the 505 alloys. Similar nomenclature is used for 515 and 1015 alloys. Composition shown is nominal for ease of understanding.

Designation	Nominal alloy content (wt%)					Intercritical anneal		Carbide tempering	
	Mn	C	Si	Al	Mo	Temp (°C)	Duration (h)	Temp (°C)	Duration (h)
505-ICA600-1	5	0.05	0.2	0.2	. . .	600	1	. . .	. . .
A505-ICA600-20	5	0.05	0.2	0.2	. . .	600	20	. . .	. . .
505M-ICA600-1	5	0.05	0.2	0.2	0.5	600	1	. . .	. . .
505M-ICA600-20	5	0.05	0.2	0.2	0.5	600	20	. . .	. . .
505-ICA600-1-T204	5	0.05	0.2	0.2	. . .	600	1	204	2
505-ICA600-20-T204	5	0.05	0.2	0.2	. . .	600	20	204	2
505M-ICA600-1-T204	5	0.05	0.2	0.2	0.5	600	1	204	2
505M-ICA600-20-T204	5	0.05	0.2	0.2	0.5	600	20	204	2
505-ICA600-1-T530	5	0.05	0.2	0.2	. . .	600	1	530	2
505-ICA600-20-T530	5	0.05	0.2	0.2	. . .	600	20	530	2
505M-ICA600-1-T530	5	0.05	0.2	0.2	0.5	600	1	530	2
505M-ICA600-20-T530	5	0.05	0.2	0.2	0.5	600	20	530	2
505-ICA650-1	5	0.05	0.2	0.2	. . .	650	1	. . .	. . .
505-ICA650-20	5	0.05	0.2	0.2	. . .	650	20	. . .	. . .
505M-ICA650-1	5	0.05	0.2	0.2	0.5	650	1	. . .	. . .
505M-ICA650-20	5	0.05	0.2	0.2	0.5	650	20	. . .	. . .
505-ICA650-1-T204	5	0.05	0.2	0.2	. . .	650	1	204	2
505-ICA650-20-T204	5	0.05	0.2	0.2	. . .	650	20	204	2
505M-ICA650-1-T204	5	0.05	0.2	0.2	0.5	650	1	204	2
505M-ICA650-20-T204	5	0.05	0.2	0.2	0.5	650	20	204	2
505-ICA650-1-T530	5	0.05	0.2	0.2	. . .	650	1	530	2
505-ICA650-20-T530	5	0.05	0.2	0.2	. . .	650	20	530	2
505M-ICA650-1-T530	5	0.05	0.2	0.2	0.5	650	1	530	2
505M-ICA650-20-T530	5	0.05	0.2	0.2	0.5	650	20	530	2

The γ phase content was measured through X-ray diffraction (XRD) using a Bruker D2 Phaser diffractometer with a cobalt radiation source operating at a voltage of 30 kV and current of 10 mA. Scans were carried out with a 2θ of 45° to 105°, a 0.02° step size, and integrating for 1 s per step. Phase quantification was performed using Rietveld refinement through the TOPAS software.

The microstructure and phase morphology were identified with a ThermoFisher Apreo S using an EDAX Velocity detector. Electron backscattered diffraction (EBSD) scans were performed at an accelerating voltage of 20 kV and a working distance of approximately 12 mm. Measurements were performed with a scan step size of 400 nm on a hexagonal grid. The resulting EBSD maps were analyzed using the MTEX package in MATLAB. From the EBSD orientation maps, the prior γ grains were reconstructed using a graph clustering algorithm.[7,8]

Sub-sized flat ASTM E8[9] tensile bars with gauge length of 25 mm and gauge width of 6 mm were electro-discharge machined (EDM) parallel to the rolling direction and tested to understand the effect of heat treatment and γ content on the tensile behavior of the alloy. Strain was measured using digital image correlation (DIC), and tests were performed in displacement control at a rate of 0.01 mm/s using a 250-kN load cell on an Instron model 5989 frame. After fracture the cross-sectional area was measured and the reduction in area (RA) was calculated using Eq. 2, where A_0 is the initial cross section and A_f is the cross section after testing and fracture.

$$RA = \ln \frac{A_0}{A_f} \tag{2}$$

Characterization and testing were performed in a series of screening steps. Initially, hardness and γ content were measured on all alloys and heat treatment combinations. From these results, a second round of screening was performed by CVN testing at –40 °C using full-size samples in accordance with ASTM E23.[10] Two final heat treatment conditions were selected from each alloy for full characterization including quasi static tensile testing and CVN from –80 to 60 °C in the transverse-longitudinal orientation such that the principal stress was normal to the rolling direction.

3. Results and Discussion

3.1 Screening: ICA Effect on γ Stabilization

The purpose of the ICA treatment was to partition C and stabilize γ. Successful partitioning can be observed as an increase in the volume percent of γ and may also be accompanied by a change in hardness. The ICA effect on γ volume percent and alloy hardness prior to secondary tempering is shown in Fig. 2. For each unique

alloy the γ content and hardness are generally inversely related (Fig. 2a). This is understood in the context that γ is the softer phase in the dual-phase microstructure. The 505, 505M, 515, and 515M alloys have significantly less γ than the 1015 and 1015M alloys. The 1015 and 1015M alloys also have the highest hardness, with the 505 and 505M alloys generally being the softest.

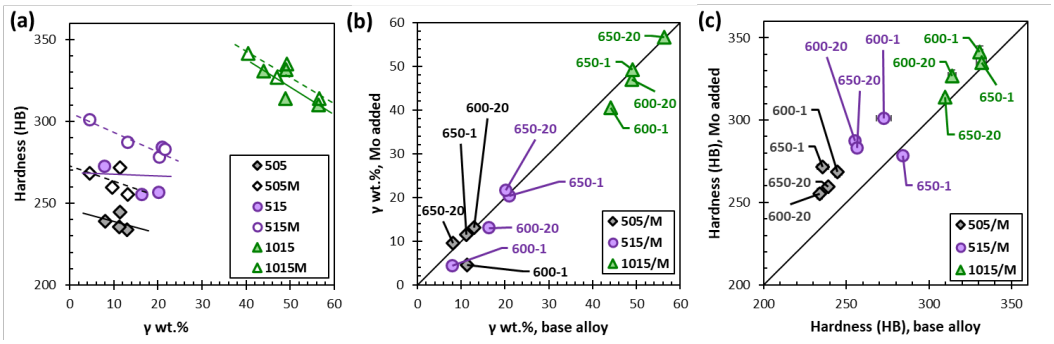

Fig. 2 Hardness and γ content of alloys after ICA treatment and prior to secondary tempering. (a) Hardness as a function of γ volume percent by alloy, linear trend lines for each alloy shown to guide the eye only. Comparison of base alloy and Mo-modified alloys for (b) γ volume percent and (c) hardness.

The ICA treatment had the smallest effect on the 505 and 505M alloys because there are lower concentrations of substitutional and interstitial elements that stabilize the γ (C and Mn) compared to the 515, 515M, 1015, and 1015M alloys. Figure 2a shows that for the 505 alloy, there was little change in the hardness or γ volume percent for the four different ICA treatments, whereas there is a greater variation for the 505M alloys.

Increasing C content would be expected to increase γ stabilization during the ICA treatment. This is observed in Fig. 2b as the γ volume percent of alloy 515 and 515M alloys is approximately double that of the 505 and 505M alloys after 650 °C ICA. However, Fig. 2b shows that for the 600 °C ICA treatment, there is no significant difference in γ volume percent between the 505 and 515 alloys, suggesting insufficient partitioning occurred at 600 °C to stabilize γ. This effect is understood to be due to an incomplete stabilization of the γ as reported by Field et al.[4] for a nominally 5Mn–0.2C (wt%) steel. Despite the similar γ volume percent after the 600 °C ICA, alloy 515 has a higher hardness than alloy 505, with the highest hardness observed for the shorter (1 h) ICA times. This suggests that the higher C level in the 515 alloy initially results in a stronger α, and as C partitions to γ this strength level is reduced.

Figures 2a and b show that the 1015 and 1015M alloys, which have the highest fraction of the γ-stabilizing elements Mn and C, have the greatest fraction of γ regardless of ICA temperature. Like the 515 and 515M alloys, the highest hardness

is observed for shorter ICA times. Unlike the 505 alloy, γ volume percent increases with increasing ICA time and temperature for the 515 and 1015 alloys, suggesting that higher Mn and C content enabled more partitioning to stabilize γ during annealing.

Compared to their respective base alloys in the same ICA condition, the Mo-modified alloys generally had a slightly decreased γ volume percent (Fig. 2b) and a higher hardness (Fig. 2c). The addition of Mo at a fixed alloy and ICA treatment leads to a direct decrease in the measured γ. This potentially indicates that the formation of carbides after alloying with Mo within the investigated steels reduces the available C to stabilize the γ. It is also noted that the loss of γ by alloying with Mo was less significant after the 650 °C ICA treatment. This is a result of reduced Mo_2C stability with increasing temperature. By forming less of the carbide at 650 °C, the carbon potential in the γ is increased, allowing diffusion to the growing γ for an enhanced γ stability.

Mo additions to the alloy increased the hardness at all points in the heat treatment. This hardness increase is attributed to either solid solution strengthening by the addition of Mo or by the formation of fine carbides. Further work involving transmission electron microscopy (TEM) is needed to fully identify the mechanism for the increase in strength. Interestingly, the 1015/M alloys, which have the highest γ content of the alloy classes investigated here, also have the highest hardness. There is very little variation in the formed γ after the different ICA treatments, with an average γ concentration of 50 ± 5%.

Representative microstructures of the base alloys as depicted by EBSD phase maps are included in Fig. 3. The morphology of the precipitated γ changes with composition and ICA temperature. For the 505 base alloy, fine γ particles are found along the grain boundaries; after the 600 °C ICA the γ is more globular as compared to the more lamellar morphology after the 650 °C ICA treatment. In the 515 base alloy, the shape of the γ is unchanged with the ICA treatment temperature while the quantity of γ is greatly increased at 650 °C as compared to 600 °C, in agreement with the XRD results. Similarly, for the 1015 base alloy the morphology of the γ is consistent regardless of ICA temperature while the amount of γ increases with ICA temperature. The relative γ content measured with EBSD is also consistent with the XRD results.

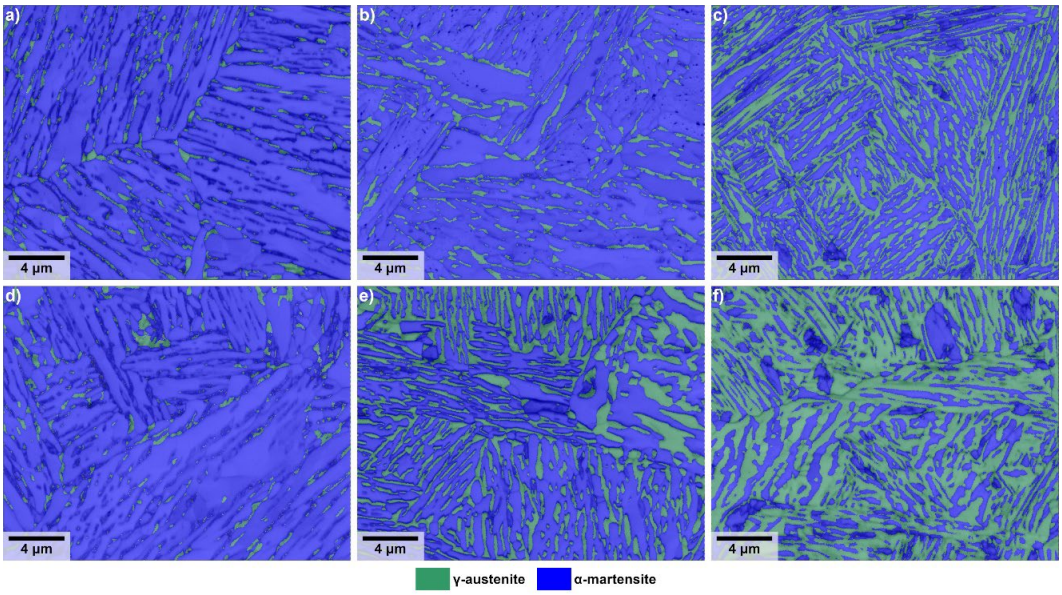

Fig. 3 Representative EBSD phase maps for the (a) 505, (b) 515, and (c) 1015 base alloys after ICA at 600 °C for 20 h Additional representative EBSD phase maps for the (d) 505, (e) 515, and (f) 1015 base alloys after ICA at 650 °C for 20 h. All phase maps are shaded by the band contrast, which highlights fine features within the phase maps.

Additional analysis of the EBSD maps was performed to reconstruct the prior γ grains. A representative example of the prior γ reconstruction for the 505-ICA600-24-T204 condition is shown in Fig. 4. The orientation map of the α-martensite structure shows how grains with similar orientations are grouped into prior γ grains. The prior γ orientation reconstruction indicates that a significant number of annealing twins are present in the prior γ structure. However, this may also be a consequence of the difficulty distinguishing the twinned and untwinned orientation for a given α orientation due to the high symmetry of the parent-child orientation relationship.

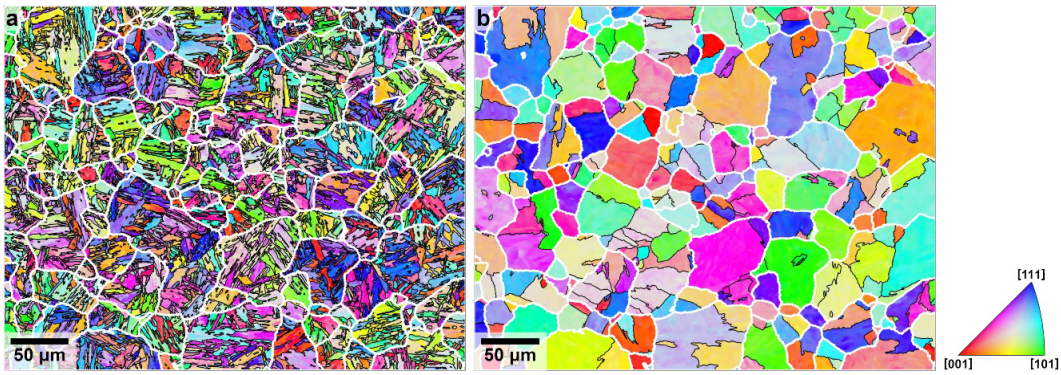

Fig. 4 Representative reconstruction of the prior γ microstructure for the 505 base alloy annealed at 600 °C for 20 h was calculated from the α-martensite and retained γ orientations. An orientation map of α-martensite with the prior γ grain boundaries indicated as thick white boundaries is shown in (a) while the reconstructed prior γ orientations with the prior γ grain boundaries indicated as thick white boundaries is shown in (b).

3.2 Screening: Carbide Temper Effect

The carbide temper had a varying effect depending on the ICA treatment and alloying elements, and a not insignificant effect on the base alloys as shown in Figs. 5a–c. In the 505 alloy, tempering after a 600 °C ICA led to a decrease in hardness, with no significant change in γ volume percent. For tempering of the 505 alloy after ICA650-1, an increase in γ with no change in hardness was observed. The only ICA temper combination that affected both hardness and γ volume percent in the 505 base alloy was the ICA650-20 followed by the 530 °C temper. Whereas tempering the 505 base alloy generally affected the γ volume percent more than the hardness, tempering the 515 base alloy had a larger effect on the hardness than the γ volume percent. Tempering 515 after a 600 °C ICA resulted in a decrease in γ volume percent with no significant change in hardness. The 650 °C ICA again had varying results in the 515 alloys, with tempering the ICA650-1 condition leading to decreased hardness with similar γ volume percent and tempering the ICA650-20 condition having little effect on either hardness or γ volume percent. Tempering the 1015 base alloy led to slight decreases in γ volume percent and minimal changes in hardness, except for tempering the ICA650-1 condition, which had little significant change.

Tempering of the Mo-modified alloys has a more pronounced effect on hardness than the base alloys, as shown in Figs. 5d–f. In the 505M alloy, tempering at 530 C decreased the hardness when preceded by a 650 °C ICA treatment. Tempering 505M had little hardness effect for other ICA and temper combinations. The 515M alloy had decreased hardness after tempering at 530 °C when the ICA treatment was held for 20 h. An increase in hardness was observed for the 204 °C temper of the 515M-ICA650-1 treatment. Tempering the 1015M alloy had no significant effect when preceded by ICA at 600 °C, or for short ICA treatment times.

Tempering the 1015M-ICA600-20 condition with a 530 °C temper resulted in decreased hardness and increased γ. Tempering the 1015M-ICA650-20 condition led to decreased hardness and decreased γ for both 204 and 530 °C tempers.

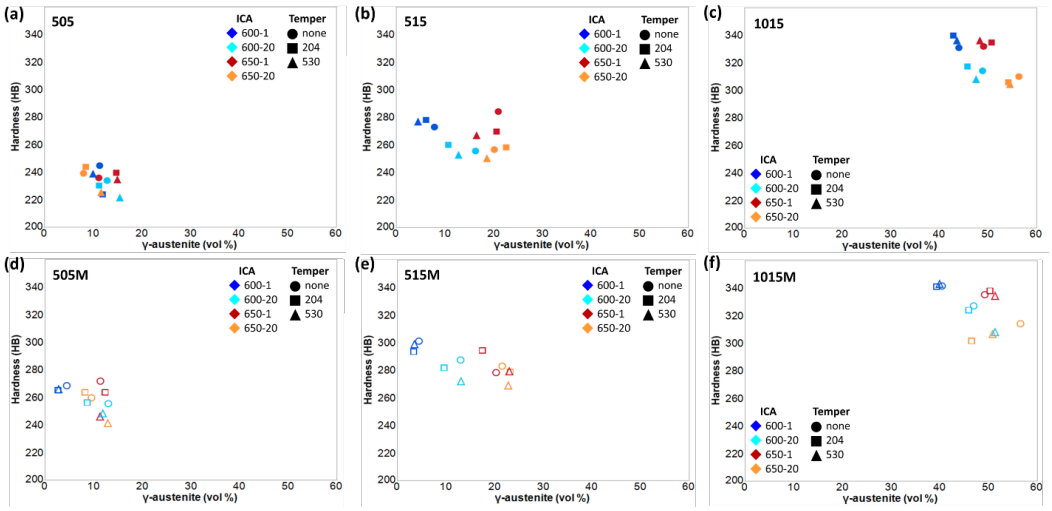

Fig. 5 Hardness as a function of γ content resulting from various ICA and temper treatments for base alloys (a) 505, (b) 515, (c) 1015 and Mo-modified alloys (d) 505M, (e) 515M, and (f) 1015M

To better assess the influence of Mo modification on carbide tempering response, the change in hardness and γ volume percent between comparable ICA and temper combinations is shown in Fig. 6. In the 505 and 505M alloy, Mo additions increased hardness and generally decreased γ volume percent. Tempering 505M always resulted in a net decrease in γ volume percent. Tempering 505M for ICA600 always resulted in a net increase in hardness, whereas tempering 505M for ICA650 resulted in a net decrease in hardness. In the 515 and 515M alloys, Mo additions increased hardness except for the untempered ICA650-1 treatment. Tempering 515M-600 conditions led to a net decrease in hardness and a net increase in γ volume percent. Tempering 515M-ICA650 conditions led to a net decrease in γ volume percent for 204 °C tempers and an increase in γ volume percent for 530 °C tempers. Tempering the 515M-ICA650-20 condition was a net decrease in hardness, but tempering 515M-ICA650-1 resulted in a net increase in hardness compared to tempering the 515 base alloy. Mo additions to the 1015 alloy generally increased hardness, except for a few tempered conditions. Tempering 1015M-ICA600 conditions resulted in a net decrease in hardness, accompanied by a net increase in γ volume percent for the ICA600-20 treatment. Similarly, tempering 1015M-ICA650 resulted in a net decrease in hardness; however, for the ICA650-20 treatment this was also accompanied by a decrease in γ volume percent.

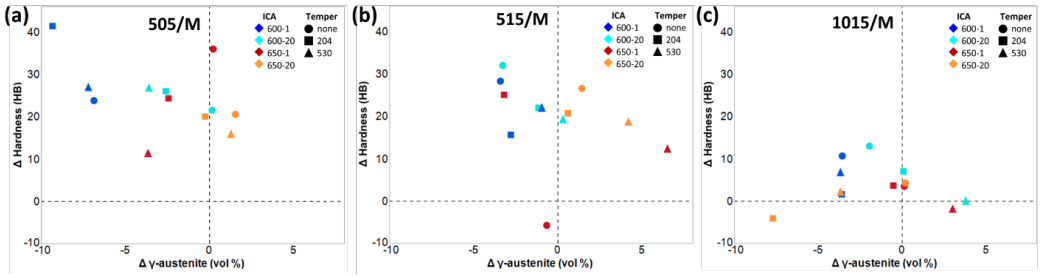

Fig. 6 Difference in hardness and γ volume fraction between base alloy and Mo-modified alloy after tempering for (a) 505/M, (b) 515/M, and (c) 1015/M alloys.

3.3 Screening: Charpy V-Notch Results

To identify heat treatments of interest for further testing, an initial subset of the heat treatments were applied to the six alloys and tested using CVN toughness testing at –40 °C. Material limitations restricted this testing to a maximum of three conditions per alloy. The most interesting conditions were selected to allow for comparisons to be made across the multivariable domain. The results of the impact testing are shown relative to the γ content in Fig. 7a and relative to the hardness in Fig. 7b with the MIL-DTL-12560K[11] specification line shown in reference. The data provided is tabulated and shown in Table 3. Figure 7a shows most of the Mo-modified alloys had higher impact toughness than their base alloy counterparts for similar γ volume fractions. The most significant finding of these results was that by alloying with Mo and proper tempering, both strength and toughness were increased, which is an atypical response for metals. This effect is generally seen in Fig. 7b and can be clearly shown when comparing the tabulated values of 505 and 505M after the same ICA treatment of 20 h at 600 and 650 °C. The 505M, when tempered at 204 °C, increases the toughness by 20 ft-lb with an increase in hardness of 22 HBW. More significantly, the 650 °C ICA condition exhibits an 87 ft-lb increase with an associated 25 HBW. The same trend is observed in all modified alloys with the addition of the carbide temper treatment at 530 °C. This is indicative of the efficacy of Mo improving toughness of these medium-Mn steels.

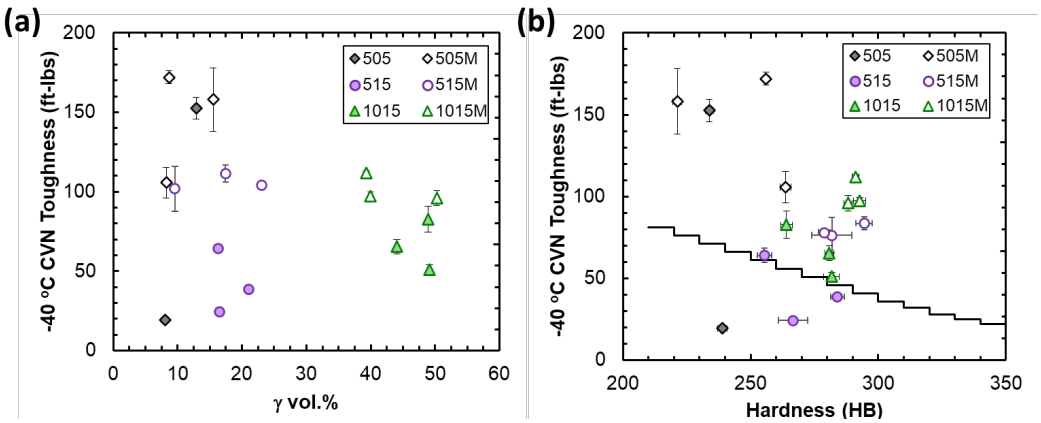

Fig. 7 Initial CVN toughness screening of properties as a function of (a) γ volume percent and (b) hardness

Table 3 Data from subset testing, with final heat treatments for each alloy shown in bold

Alloy	ICA temp (°C)	ICA time (h)	Carbide precipitation (°C)	γ (vol%)	Hardness (HBW)	CVN energy (ft-lb)
505	**600**	**20**	…	**13**	**204 ± 2**	**153 ± 19**
	650	**20**	…	**8**	**209 ± 2**	**19 ± 1**
505M	**600**	**20**	**204**	**9**	**226 ± 1**	**172 ± 4**
	600	20	530	16	191 ± 2	158 ± 20
	650	**20**	**204**	**8**	**234 ± 2**	**106 ± 10**
515	**600**	**20**	…	**16**	**225 ± 3**	**64 ± 4**
	650	**1**	…	**21**	**254 ± 3**	**39 ± 1**
	650	1	530	17	237 ± 6	24 ± 2
515M	600	20	204	10	252 ± 8	76 ± 11
	650	**1**	**204**	**17**	**265 ± 3**	**84 ± 4**
	650	**1**	**530**	**23**	**249 ± 2**	**78 ± 2**
1015	600	1	…	44	301 ± 2	49 ± 3
	600	**20**	…	**49**	**284 ± 2**	**62 ± 6**
	650	**1**	…	**49**	**302 ± 3**	**38 ± 2**
1015M	**600**	**1**	**204**	**39**	**311 ± 1**	**84 ± 1**
	600	1	530	40	313 ± 2	73 ± 2
	650	**1**	**204**	**50**	**308 ± 2**	**72 ± 4**

A final set of two heat treatment conditions were selected for each alloy for further examination via CVN testing as a function of temperature and quasi-static tension testing. The conditions used are highlighted as bold in Table 3. Selection was performed to compare the stability and toughening effects of various concentration of γ at near similar hardness levels.

3.4 Final: Charpy V-Notch Temperature-Dependent Results

The impact behavior of the final heat treatments was investigated as a function of temperature to identify a ductile-to-brittle transition temperature (DBTT). CVN impact testing was performed at temperatures ranging from –80 to 60 °C. Only alloy conditions with room temperature (nominally 23 °C) impact energies below 150 ft-lb were tested at 60 °C due to equipment limitations. The effect of temperature on toughness is shown in Fig. 8. For clarity, discussion of the results is separated by alloy family.

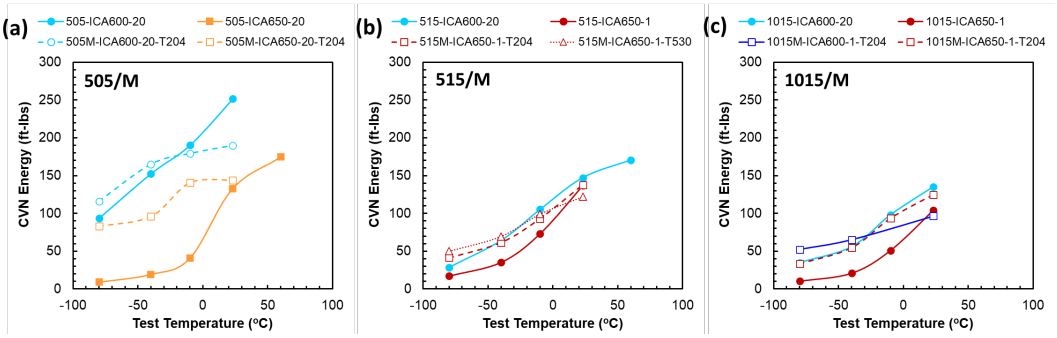

Fig. 8 Impact properties as a function of testing temperature for the (a) 505/M, (b) 515/M, and (c) 1015M alloys. Base alloys are shown with solid lines and filled symbols, Mo-modified are shown with dashed lines and open symbols.

3.4.1 505/505M Alloy

The temperature-dependent CVN results provide further insight into the complex effect of Mo on the impact toughness of the 505 alloy family. The ICA600-20 treatment results in higher toughness than the ICA650-20 treatment across the range of temperatures tested. The Mo-modified alloy has increased low-temperature toughness and decreased high-temperature toughness compared to the base alloy for both ICA treatments, resulting in a smaller change between the upper and lower shelf energies. The DBTT is also shifted to lower temperatures from 0 °C to –30 °C for the Mo-modified alloys. The effect of Mo is more pronounced for the ICA650-20 treatment, with an increase of approximately 70 ft-lb at each of the subzero temperatures tested. At room temperature, however, both the Mo-modified and base 505 alloy had nominally similar toughness (144 ± 4 and 133 ± 10 ft-lb, respectively). For the ICA600-20 treatment, Mo modifications only had a significant effect on raising the toughness at –80 °C (100 → 120 ft-lb) and showed a significant decrease in toughness at room temperature (252 ± 20 vs. 190 ± 15 ft-lb).

The change in toughness response for the different ICA treatments and Mo modifications is a function of the γ concentration. The 505 after ICA600-20

contains 15 vol% γ while the 505M after the same treatment and a 204 °C carbide temper only contains 9 vol% γ. The lower quantity of γ in the structure is considered more stable as was reported by Field et al.[4] They showed that as the quantity of γ increases the mass balance of γ-stabilizing elements needs to decrease within that γ. This leads to a less thermally or mechanically stable γ that can transform before the initiation of the test during cooling to the lower test temperatures. The transformation proceeding from the test produces fresh brittle martensite, which is known to create a less fracture-resistant structure and lowered CVN performance. The alloys with higher γ content, and therefore less stable γ, appear to have a distinct shift in the absorbed energy as the testing temperature increases. The alloy conditions with especially low –80 °C toughness and less than 18 ft-lb (i.e., 505-ICA650-20, 515-ICA650-1, and 1015-ICA650-1) all undergo a significant increase in toughness at room temperature. It is significant to note that there is on average a nine-times increase in toughness for the alloy that produced the lowest –80 °C toughness. For the other three conditions within the 505-alloy family, only a one- to two-times increase in toughness is observed going from the –80 °C condition to room temperature. The difference in response is understood vis-á-vis the γ stability; below a certain temperature threshold the γ is too unstable and produces conditions for brittle fracture. At the higher testing temperature where the γ is still stable, however, the greater volume of γ becomes more beneficial and produces greater energy absorption capacity.

3.4.2 515/515M Alloy

The impact behavior of the 515-type alloys was not significantly altered through heat treatment modification. The effect of ICA (650 vs. 600 °C) produced an increase in toughness as ICA temperature was decreased, consistent with what Field et al.[4] showed for a comparable alloy of 5Mn–0.20C–bal. Fe (in weight percent) processed in a similar manner and heat-treated to a similar condition. This is associated with the γ stability. As the ICA treatment temperature increases, the volume fraction of γ increased thereby diluting the stabilizing elements and weakening both the mechanical and thermal stability of the γ. This is best illustrated when comparing the ICA650-1 and ICA600-20 that contain 12 versus 19 vol% γ, respectively. The lower measured γ ICA650-1 condition has an 80% increase in –40 °C CVN toughness.

For the Mo-modified alloy, the heat treatment approach was different from what was done with the 505-type alloys and noted previously. When comparing the base alloy to the low-temperature carbide tempered condition (204 °C), an average of 20 ft-lb increase is observed at testing temperature less than or equal to –10 °C. At room temperature 515 and 515M carbide tempered at 204 °C are indistinguishable

(136 ± 5 vs. 138 ± 1 ft-lb). The increase in carbide tempering from 204 to 530 °C leads to a moderate increase in toughness of approximately 8 ft-lb at all test temperature less than or equal to –10 °C. While this is a moderate increase in toughness, it is also associated with a 5% increase in the strength of the steel, which is a significant synergistic improvement in toughness and strength.

3.4.3 1015/1015M Alloy

The effect of ICA treatment temperature on the base 1015 alloy is similar to what was observed in the 505 and 515 base alloys. An increase in the ICA treatment leads to a reduction in toughness. The effect of ICA treatment on the CVN toughness is similarly observed in the 1015M alloy. For the two non-Mo containing conditions, 1015-ICA600-20 and 1015-ICA650-1, the difference in γ concentration is inconsequential (48.9 vs. 49.1 vol%, respectively). However, the 1015-ICA600-20 exhibits an impact energy that is two to three times greater than the 1015-ICA650-1 condition. This is an interesting result relative to the γ concentration and requires further study to identify the cause for the increase in toughness. However, the 1015-ICA600-20 condition exhibits a great reduction in area as measured after quasi-static tensile testing and is discussed in greater detail in Section 3.5.3.

The addition of Mo produces a significant increase in strength and toughness in the base 1015 alloys. The highest low-temperature toughness is obtained in the 1015M-ICA600-1-204T condition, which contains the lowest γ concentration of 39 vol%. For all of the 1015-type alloys, however, the toughness does not increase dramatically as the test temperature rises. This is potentially understood as being a function of the γ stability. As such, even at the sub-ambient testing temperatures the γ does not transform leading to no significant change in the microstructure as a function of temperature. This was noted previously in Section 3.4.1.

The 1015M-ICA650-1-204T has the highest γ concentration (50.3 vol%); however, the toughness is not as significantly degraded as that observed in the previously noted alloys. The high γ concentration does lead to a 20 ft-lb drop in toughness at –80 °C from the superior 1015M-ICA600-1-204T condition but it is not as low as the 1015-ICA650-1 condition (10 ft-lb). In addition, the 1015M-ICA600-1-204T toughness is equivalent to the best performing base alloy 1015-ICA600-20 with a slightly higher γ concentration (50.3 vs. 49.1 vol%). This implies that the Mo addition does provide some toughening that offsets the deleterious effect of γ on the low-temperature toughness of medium-Mn steels. The 1015M alloy after 600 °C and 204 °C carbide temper had the highest yield strength with significant work hardening observed during quasi-static testing.

3.5 Final: Tensile Behavior

The stress–strain response of the steels is shown in Fig. 9. The tensile response of the alloy was interrogated to determine the yield and ultimate strength of the alloys as a function of the final heat treatment. The quasi-static tensile tests were also performed to understand the work-hardening behavior and ductility of the steels, which are described in greater detail in Section 3.6. The tabulated mechanical behavior is provided in Table 4, with the prior γ grain size as measured according to EBSD.

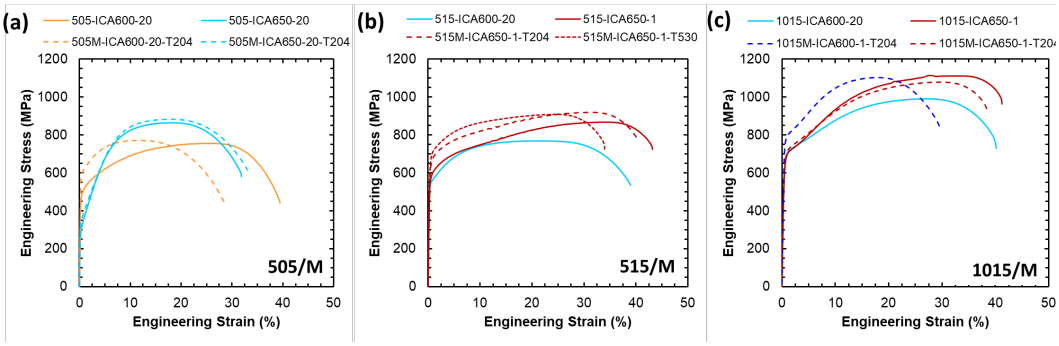

Fig. 9 Quasi-static tensile behavior of the (a) 505/M, (b) 515/M, and (c) 1015/M alloys

Table 4 Mechanical property values as measured from quasi-static testing

Alloy	ICA temp/time (°C-h)	Carbide precipitation (°C)	Yield strength (MPa)	Ultimate strength (MPa)	Uniform elongation (%)	Total elongation (%)	Reduction in area (true)	Prior γ grain size (μm)
505	600-20	…	470 ± 14	755 ± 2	25.9 ± 0.1	39.5 ± 0.1	1.28 ± 0.01	53 ± 21
	650-20		305 ± 7	866 ± 1	17.7 ± 0.9	30.9 ± 1.4	1.22 ± 0.10	54 ± 12
505M	600-20	204	600 ± 5	771 ± 1	11.3 ± 0.1	23.8 ± 6.5	1.37 ± 0.02	79 ± 40
	650-20	204	340 ± 1	887 ± 5	17.5 ± 0.1	33.0 ± 0.1	1.09 ± 0.02	51 ± 29
515	600-20	…	543 ± 4	772 ± 3	20.6 ± 1.1	38.2 ± 1.1	1.13 ± 0.03	49± 16
	650-1		560 ± 1	867 ± 1	33.6 ± 0.8	43.2 ± 0.1	0.85 ± 0.05	63 ± 24
515M	650-1	204	635 ± 7	920 ± 1	29.9 ± 1.5	38.7 ± 2.4	0.85 ± 0.05	39 ± 17
	650-1	530	668 ± 4	908 ± 2	24.4 ± 0.6	34.3 ± 04	0.86 ± 0.06	57 ± 26
1015	600-20	…	628 ± 4	993 ± 2	26.5 ± 0.1	39.5 ± 0.9	0.92 ± 0.03	45 ± 19
	650-1		610 ± 14	1115 ± 1	28.9 ± 1.3	39.0 ± 3.2	0.78 ± 0.04	39 ± 14
1015M	600-1	204	730 ± 14	1104 ± 1	17.7 ± 0.4	28.7 ± 1.1	0.76 ± 0.07	26 ± 16
	650-1	204	628 ± 4	1077 ± 4	29.4 ± 0.2	38.0 ± 0.6	0.74 ± 0.06	36 ± 16

3.5.1 505/505M Alloy

As would be anticipated the low-C, low-Mn alloys (505 and 505M) both exhibit the lowest yield strengths. These alloys, however, also produce the highest post-necking ductility as measured by reduction in area. The effect of Mo addition plus the tempering step shows the greatest change in properties occurs between the

505-ICA600-20 and the 505M-ICA600-20-204T with a 130-MPa increase in the yield strength with a minimal change in the ultimate tensile strength of the material. The 505-ICA600-20 exhibits a greater degree of work hardening from the lower initial yield strength to the equivalent ultimate strength. The lower yield strength of the 505-ICA600-20 is attributed to the higher volume fraction of γ (16 vs. 9 vol%) while the greater content of γ provides an increased capacity for the TRIP effect leading to a greater total ductility during the quasi-static tension tests. The 505M-ICA600-20-204T has a significantly reduced total elongation with a 15% relative decrease in both the total and uniform elongation as compared to the base alloy with the same heat treatment. However, the increment of strain beyond uniform elongation (i.e., post-necking elongation) is similar for both alloys with a difference of 0.7% strain. This is further corroborated by the fact that they both are measured to have similar total reduction in area.

In the 505M-650-20-204T, as compared to the 505-650-20, the addition of Mo leads to moderate yield strength increases without any significant change in the ultimate strength or change in elongation response. The measured γ concentration between these two conditions is measured to be the same, 14 vol%. This would further corroborate the effect of γ on the yield response as discussed previously on the γ content relative to the initial yielding behavior. There is a slight increase in the yield strength however from the Mo plus temper state and the possibility for some solid solution strengthening to the alloy.

3.5.2 515/515M Alloy

The base alloy comparison was done at two different ICA treatments with both temperature and time varied. The longer time was used on the lower temperature to allow γ-stabilizing elements to diffuse and reach near equilibrium, and a shorter time was used at the 650 °C ICA treatment. They produced similar γ concentrations: 6 vol% for the 600 °C 20-h treatment and 21 vol% for the 650 °C 1-h treatment. These two treatment combinations were chosen to identify if at equivalent tempering parameters as calculated by the Holloman-Jaffe tempering parameter (T_p)[12] shown in Eq. 3, they would produce similar properties.

$$T_p = T * (\log t + C) \tag{3}$$

where T is the temperature in kelvin, t is time in hours, and C is a constant typically ranging from 15 to 20. While the yield strengths were very similar, the ultimate tensile strength and ductility were observed to be higher in the ICA650-1 condition compared to the ICA600-20 state. This is attributed to the higher volume fraction of γ in the ICA650-1 treatment and higher work hardening producing an approximately 100 MPa increase in ultimate strength. This is assumed to be

evidence of the TRIP effect where γ transforms to α-martensite during straining. TRIP is a well-documented phenomenon in steels of this class.[13] The increase in work hardening and the activation of a greater volume for TRIP behavior is also accompanied with a decrease in post-necking ductility and total reduction in area similar to what Lloyd et al.[14] showed for high-Mn TWIP and TRIP steels.

For the Mo-modified alloy, the effect of the carbide temper temperature on properties is evaluated relative to the ICA650-1 base state. After the 204T carbide temper there is a 13% increase in the yield strength and a 6% increase in the ultimate strength. This is accompanied by a 10% reduction in both the total and uniform elongation; however, the total reduction in area is not significantly altered (–0.4%). At these lower temperature tempers the ε-carbide ($M_{2.2}C$) is the transition carbide anticipated to form and is considered an effective strengthening agent that is not deleterious to the toughness of the steel. There is also the possibility of M_2C η-carbide rich in Mo. However, without TEM analysis this is not verified and is a topic for further investigation. When the tempering treatment was increased to the 530T, there is a mixed effect on strength. The yield strength is increased 19% from the base 515-ICA650-1 and 5% from the 515M-ICA650-1-204T. There is a slight change in the ultimate strength of 18 MPa; however, this is not considered significant. There is a similar loss in total and uniform elongation relative to the 515M-ICA650-1-204T condition. However, there is an increase in the post-necking ductility and the reduction in area (relative 12% and 1% change, respectively) that is associated with the highest low-temperature toughness. It is assumed that this treatment does produce the requisite η-carbide and would be consistent with Nakamura et al.'s results[5] on the high-C steel alloys. Relative to γ volume fraction and stability, the 515M-ICA650-1-530T samples contain the highest γ concentration of the 515-type alloys.

3.5.3 1015/1015M Alloy

The 1015 and 1015M alloys exhibit the highest work hardening and ultimate strength of all alloy and heat treatment condition combinations. With the higher Mn content, these alloys produce the highest γ concentrations and the greatest work hardening compared to the lower Mn steels. When examining the base 1015 alloy, the effect of different ICA treatment time and temperature combinations with a constant T_p were interrogated. At roughly equal γ concentrations (~49 vol%) these alloys have the highest concentration of γ for all the alloys and conditions subjected to tension testing. The two ICA treatments produce statistically equivalent yield strengths. The higher temperature ICA treatment does produce a greater degree of work hardening leading to a slight increase in the ultimate tensile strength. However, the measured increase is small, approximately 25 MPa. The largest

difference is in the reduction in area with a relative difference of 15%, which is discussed in greater detail relative to the CVN toughness of the steel in Section 3.6.

The carbide tempering on the Mo-containing alloys produces mixed results for the high-Mn steel. The effect appears to be a function of the prior ICA treatment and the γ concentration developed therein. The 1015M-ICA600-1-204T produces a 100-MPa increase in yield strength with a negligible change in the ultimate strength. However, this could be due to the reduction in γ content from the base 1015 conditions (39 vol%). Section 3.1 discusses how increases in the γ concentration can lead to a decrease in the initial yielding response. This theory is further supported by the 1015M-ICA650-1-204T in that a γ concentration of 50 vol% has a yield strength similar to that observed in the 1015-base alloys with similar γ concentrations.

3.6 Discussion: Toughness and Ductility Relationship

The reduction in area is a significant measure of a materials ability to accommodate plastic strain and its damage tolerance. While the total ductility, as measured according to the engineering strain to failure, varies significantly between alloys and heat treatments, the reduction in area appears to be consistent to certain features. The low-C, 5Mn alloys (505 and 505M) exhibit the highest reduction in area of all the alloys. This is associated with the greatest post-necking ductility. The 10-Mn alloys (1015 and 1015M) exhibit the lowest post-necking elongation and reduction in area. The 515 and 515M alloys lie between.

It is interesting to consider that most alloying strategies for medium-Mn steels attempt to optimize for the greatest quantities of γ through heat treatment: producing the greatest volume of γ to delay the onset of necking by the TRIP mechanism. However, total elongation and total ductility are not good measures of plasticity or damage tolerance. A material that fractures at the onset of a plastic instability (i.e., necking) in fact has lost a degree of plasticity relative to a material with the same total ductility but a large quantity of elongation post ultimate tensile strength. These concepts were addressed in the work by Field et al.,[4] which showed that the stability, not volume, of γ is most indicative of CVN toughness. Also, the sensitivity of medium-Mn steels to plastic instability was addressed vis-á-vis modeling efforts by Lloyd et al.[14] They showed that for TWinning Induced Plasticity (TWIP) and TRIP steels there is very limited post-necking elongation even when total ductility is measured to be greater than 50% strain. They postulated that this effect was caused by the material's inability to accommodate neck formation, and upon the initiation of necking the material fails. While the work by Lloyd et al.[14] investigated alloys exhibiting TWIP or TRIP responses and the

reported stress–strain behavior, the reduction in area was not typically reported. It could easily be assumed that these steels would have relatively low reduction in area due to the limited post-necking ductility.

In this work, the true reduction in area is contrasted with the –40 °C CVN toughness data. Figure 10 shows data compiled from this report as well as literature data on medium-Mn steels, high-strength steels with very high yield strength (>1100 MPa), and highly alloyed cryogenic 9 wt% Ni steels. It was found that these alloys follow an exponential relationship with a coefficient of determination (R^2) of 0.79. The authors are unaware of any direct relationship reported in literature between the quasi-static material response and the CVN impact energy of a steel. This observation further emphasizes that to improve the damage tolerance of an alloy, the reduction in area must be maximized. This is the first work to illustrate a direct relationship between quasi-static behavior and Charpy impact response across a variety of steel alloys. Also, the alloys shown here span beyond medium-Mn TRIP steels, incorporating low-alloy high-strength steels with yield strengths in excess of 1500 MPa.[15–17] With respect to medium-Mn alloys, Liang et al.[17] measured both the quasi-static and impact performance as a function of ICA temperature on a steel with a nominal composition of 0.1C–3.6Mn–bal. Fe (weight percent). They measured a peak in the –40 °C toughness that coincided with a maximum of the reduction in area and was independent of strength, both yield and ultimate, as well as total elongation.

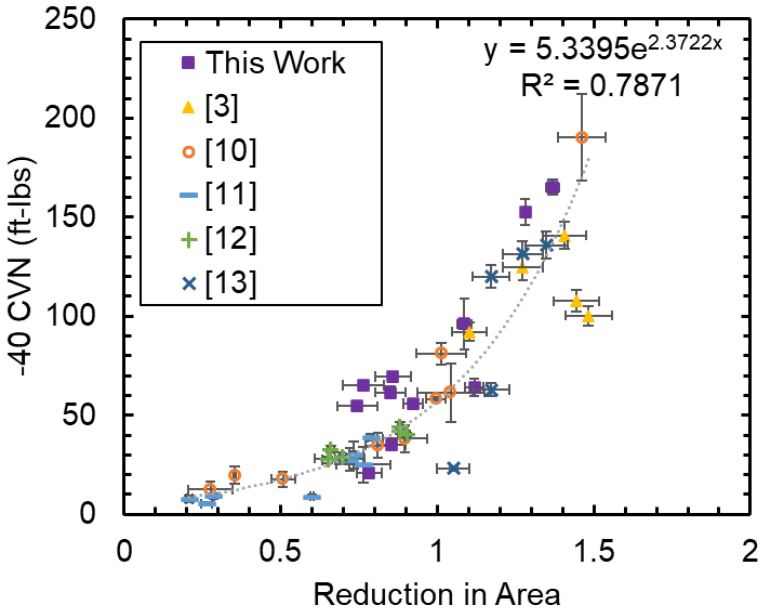

Fig. 10 True logarithmic reduction in area from quasi-static tension test relative to –40 °C CVN

3.7 Discussion: Grain Size

Interrogation of the prior γ grain size was performed to determine if there was an effect on the tensile properties of these steels. The grain size effect was correlated by the traditional Hall-Petch relationship as shown in Eq. 4:

$$Strength \propto \frac{1}{\sqrt{D(\mu m)}} \tag{4}$$

where the strength is inversely proportional to the square root of the grain size (D). To identify the effect, the grain size was graphed against the yield strength, ultimate tensile strength, and reduction in area as shown in Fig. 11. Figure 11a shows no strong correlation across alloys or even within each alloy system for the yield strength, and Figs. 11b and c show a weak correlation for the ultimate strength and reduction in area, respectively. The figure also shows as the grain size is reduced, the reduction in area decreases. These results, however, do not exclude the possibility for a Hall-Petch effect within each alloy system as there are only two data points for each alloy. This analysis was performed to determine if the Hall-Petch effect was a strong indicator for the behavior observed. It does not appear to be at this junction. To truly investigate if there is a significant contribution, a systematic variation of grain sizes would need to be intentionally produced and compared to the strength for each alloy. The relative error on the grain size measurements, as shown in Table 4, are very large though this is in part a consequence of the prior γ reconstruction process and the relatively limited data set employed.

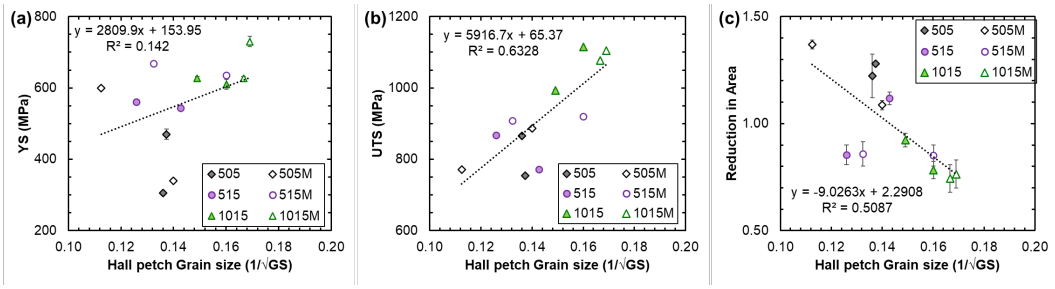

Fig. 11 Investigation of Hall-Petch relationship to (a) yield strength, YS, (b) ultimate tensile strength, UTS, and (c) reduction in area

4. Conclusion

Six medium-Mn steels with variations in C, Mn, and Mo content were investigated. The low-C, low-Mn steel modified with Mo had the highest low-temperature CVN toughness of all the steels tested in this work. Within each base alloy, the addition of Mo increased both the hardness and the CVN toughness of the alloy and provided a synergistic strengthening and toughening of the steel, which is typically unheard

of. Increases in the γ concentration were found to increase the alloy work hardening capacity due to the TRIP effect of the steels. This effect was maximized in the alloy with 10 wt% Mn that contained greater than 45 vol% γ. The quasi-static tensile behavior was related to the –40 °C CVN toughness according to the logarithmic reduction in area and was found to be related through a simple exponential relationship. This was understood to be due to the increased ability to accommodate damage and provide greater toughness as tested by the Charpy v-notch test at –40 °C. The correlation withstands scrutiny for alloys that exhibit TRIP behavior as well as high-strength steels with yield strengths in excess of 1500 MPa found in literature.

5. References

1. Field DM, Qing J, Van Aken DC. Chemistry and properties of medium-Mn two-stage TRIP steels. Metall Mater Trans A. 2018;49:4615–4632. https://doi.org/10.1007/s11661-018-4798-6.

2. Tschiyama T, Inoe T, Tobata J, Akami. Takaki S. Microstructure and mechanical properties of a medium manganese steel treated with interrupted quenching and intercritical annealing. Scripta Mat. 2016:122:36–39.

3. Niikura M, Morris JW. Thermal processing of ferritic 5Mn steel for toughness at cryogenic temperatures. Met Trans A. 1980;11:1531–1540.

4. Field DM, Magagnosc DJ, Hornbuckle BC, Lloyd JT, Limmer KR. Tailoring γ-austenite stability to improve strength and toughness of a medium-Mn steel. Metall Mater Trans A. 2022. https://doi.org/10.1007/s11661-022-06683-5.

5. Nakamura T, Shinoda T, Watanabe H. P-induced intergranular embrittlements in 2.25wt% chromium steels with variations in molybdenum and carbon contents. ISIJ Trans. 1979:19;428–434.

6. ASTM E18-17e1. Standard test methods for Rockwell hardness of metallic materials. ASTM International; 2017.

7. Niessen F, Nyyssonen T, Gazder AA, Hielscher R. Parent grain reconstruction from partially or fully transformed microstructures in MTEX. J Appl Crystallogr. 2022;55(Pt 1):180–194.

8. Hielscher R, Nyyssönen T, Niessen F, Gazder AA. The variant graph approach to improved parent grain reconstruction. arXiv preprint arXiv:2201.02103. 2022 Jan 6.

9. ASTM E8/E8M-22. Standard test methods for tension testing of metallic materials. ASTM International; 2022 July 19.

10. ASTM E23-23a. Standard test methods for notched bar impact testing of metallic materials. ASTM International; 2023 Apr 13.

11. MIL-DTL-12560K. Detail specification: armor plate, steel, wrought, homogeneous (for use in combat-vehicles and for ammunition testing). Department of the Army; 2013 Dec 7.

12. Hollomon JH, Jaffe LD. Time-temperatures relations in tempering steel. Trans Am Inst Min Metallurg Eng. 1945;162:223–249.

13. Field DM, Garza-Martinez LG, Van Aken DC. Processing and properties of medium-Mn TRIP steel to obtain a two-stage TRIP behavior. Metall Mater Trans A. 2020;51:4427–4433. https://doi.org/10.1007/s11661-020-05901-2.

14. Lloyd JT, Field DM, Limmer KR. A four parameter hardening model for TWIP and TRIP steels. Mater Des. 2020. https://doi.org/10.1016/j.matdes.2020.108878.

15. Field DM, Cluff SR, Limmer KR, Montgomery JS, Cho KC. Heat treatment and austenitization temperature effect on microstructure and impact toughness of an ultra-high strength steel. Metals. 2021;11(5):723. https://doi.org/10.3390/met11050723.

16. Field DM, Montgomery JS, Limmer KR, Cho K. Heat treatment design to modify the martensite misorientation and obtain superior strength–toughness combinations. Met Trans A. 2020;51:1038–1043.

17. Liang X, Fu H, Cui M, Liu G. Effect of intercritical tempering temperature on microstructure evolution and mechanical properties of high strength and toughness medium manganese steel. Materials. 2022;15:2162. https://doi.org/10.3390/ma15062162.

List of Symbols, Abbreviations, and Acronyms

α	ferrite
γ	austenite
Al	aluminum
ARL	Army Research Laboratory
C	carbon
CVN	Charpy v-notch
DBTT	ductile to brittle transition temperature
DEVCOM	US Army Combat Capabilities Development Command
DIC	digital image correlation
EBSD	electron backscattered diffraction
EDM	electro-discharge machined
ICA	intercritical annealing
Mn	manganese
Mo	molybdenum
N	nitrogen
Ni	nickel
O	oxygen
S	sulfur
TEM	transmission electron microscopy
TRIP	transformation-induced plasticity
TWIP	TWinning Induced Plasticity
XRD	X-ray diffraction

1 (PDF) DEFENSE TECHNICAL INFORMATION CTR DTIC OCA

1 (PDF) DEVCOM ARL FCDD RLB CI TECH LIB

5 (PDF) DEVCOM AC T GEDNEY E KUNKEL L WILLIAMS P BOUCHARD A PALAGE

2 (PDF) PEO GCS R HOWELL R NICOL

1 (PDF) USAF AFLCMC R ABRAHAMS

13 (PDF) DEVCOM ARL FCDD RLA A A RAWLETT S SCHOENFELD FCDD RLA TF L MAGNESS FCDD RLA M B CHEESEMAN K CHO FCDD RLA MD B MCWILLIAMS FCDD RLA MF K DOHERTY D FIELD K LIMMER M WALOCK M MURDOCH M RUPINEN FCDD RLA MB DJ MAGAGNOSC